Instrument Noise Calibration with Arbitrary Sensor Orientations

Zuo Zhu[*1], Siu-Kui Au[1], Xinrui Wang[1]

[1]Institute for Risk and Uncertainty and Centre for Engineering Dynamics, University of Liverpool, Liverpool, United Kingdom
[*]Corresponding author. E-mail address: zhuzuo@liverpool.ac.uk

Abstract

Instrument noise calibration is indispensable for laboratory and field testing with applications in disciplines such as seismology and structural health monitoring, establishing the basic information for the quality of data. Different methods exist assuming different kinds of information, among which the 'three-channel method' developed by Sleeman and co-workers allows one to calibrate the power spectral density (PSD) of instrument noise without prior information. The method makes use of the sample cross-covariance of three data channels assumed to measure the same input motion. In reality, the input motions of the three channels are never identical due to sensor alignment error and spatial incoherence of the input motion. This leads to bias in the estimated noise PSD, which turns out to also increase with the signal-to-noise ratio. In this paper, the noise calibration problem is investigated analytically to yield explicit formulas that account for the bias due to alignment error and spatial incoherence. Leveraging on fundamental understanding of the bias, a method is proposed which can overcome the bottleneck stemming from alignment error. The proposed method is still based on three collocated sensors but now it makes use of multi-dimensional (biaxial or triaxial) motion data. The latter is the key for the method to be applicable (unbiased) for arbitrary sensor orientations, which significantly enhances the robustness and accuracy of 'huddle test'.

Numerical studies with simulated data and a series of specially designed experiments based on servo-accelerometers are presented to verify the analytical findings, to provide a critical appraisal of the proposed method and to demonstrate practical applications.

Keywords

Instrument noise calibration; field test; huddle test; signal-to-noise ratio; alignment error; spatial incoherence

1. Introduction

Instrument noise calibration aims at determining the in-situ characteristics of the noise of data channels, which is attributed to sensor, data acquisition hardware, etc. Such information is used downstream and is therefore indispensable for many disciplines such as seismology [1-3] and structural health monitoring [4-8], establishing a baseline confidence and precision quantification for measurements. Specification and calibration certificate of instruments can provide nominal information about noise characteristics but they cannot replace in-situ calibration.

By its very nature noise is mixed with the target signal to be measured and neither one is known unless under special circumstances. Noise is commonly modelled by a stationary stochastic process and its strength is characterised by the power spectral density (PSD). An intuitively direct way to extract the noise of an instrument is to eliminate the actual vibration response from the data, which practically requires one to isolate the sensor from fixtures [9,10]. While this may not be always feasible, a common alternative is to perform a ‘huddle test’ [11-13], where multiple sensors to be calibrated are placed together to measure the same input motion. By virtue of redundant information the PSD of instrument noise can be estimated by statistical means. The ‘two-channel method’ [14] is a technique that uses two collocated and co-aligned

data channels. It requires prior information about the transfer functions of the data channels, whose error can smear into the estimated noise characteristics [15,16]. The ‘three-channel method’ [17] allows one to estimate the PSD of instrument noise without prior information. It has become one of the preferred methods [18] and was applied to calibrate a variety of sensors [19-23].

One pivotal assumption for the two- and three-channel method is that the collocated channels measure the same input motion. For this reason the channels should be oriented along the same direction. In implementation, alignment error is inevitable and it has been found in empirical studies to induce bias in the estimated noise PSD [24-26], which turns out to increase with the signal-to-noise ratio [27,28]. Some attempts [29,30] have been made to mitigate misalignment, although the fundamental issue remains unresolved.

In this work, the three-channel method is first investigated analytically (Section 2) to yield an explicit formula for the statistical bias that allows one to understand its origins. Leveraging on such understanding, a new method based on three collocated sensors but now applicable for arbitrary sensor orientations is developed in Section 3, allowing one to calibrate instruments in a more robust and accurate manner. In addition to alignment error, the effect of spatial incoherence is also investigated in Section 4. A comprehensive study based on synthetic and experimental data is presented in different sections to verify the analytical findings, to provide a critical appraisal of the proposed method and to demonstrate applications. Recommendations for the proposed method are summarised in Section 5.

2. Three-Channel method

The three-channel method assumes three collocated and co-aligned channels from three sensors (say Sensors i, j and k) measuring a common ‘input motion’, which refers to the mechanical

motion experienced by the sensor and is the target to be measured. Fig. 1 shows a schematic diagram where the circle represents the sensor and the arrow inside indicates the orientation. Assuming that the input-output relationship of the instrument is linear, the output signal x_i of Sensor i can be modelled in the time domain as the convolution of the input motion z with the impulse response g_i of Sensor i and added with the data channel noise n_i:

$$x_i = g_i * z + n_i \tag{1}$$

where '*' denotes the convolution; the dependence of quantities on time has been omitted for notational simplicity. Similar expressions can be written for other sensors. In the frequency domain, the relationship analogous to (1) is

$$X_i = G_i Z + \varepsilon_i \tag{2}$$

where X_i, G_i, Z and ε_i denote respectively the scaled Fourier transforms (FTs) of x_i, g_i, z and n_i; their dependence on frequency has been omitted for notational simplicity.

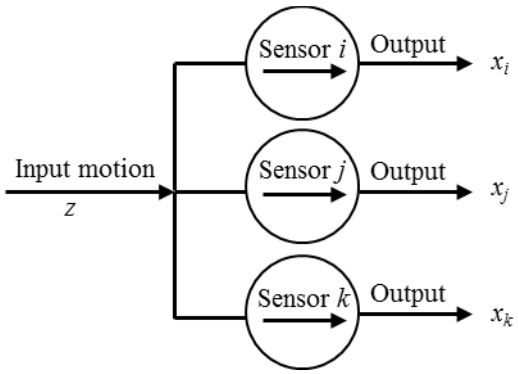

Fig. 1 Schematic diagram of the three-channel method

Modelling the input motion and instrument noise as stationary stochastic process, the cross PSD between X_i and X_k (say) is equal to $S_{ik} = E(X_i X_k^*)$ where the superscript '*' denotes the complex conjugate and $E(\bullet)$ denotes the expectation. Assuming that the instrument noise

between different channels are uncorrelated and that they are also uncorrelated from the input motion, one obtains

$$S_{ii} = G_i S_Z G_i^* + S_{ei} \tag{3}$$

$$S_{ji} = G_j S_Z G_i^* \quad S_{jk} = G_j S_Z G_k^* \quad S_{ik} = G_i S_Z G_k^* \tag{4}$$

where $S_Z = E(ZZ^*)$ is the PSD of the common input motion.

In (3)-(4), the target is to determine the noise PSD S_{ei}. While the auto and cross PSDs on the LHS (left-hand-side) can be estimated from measured data, the PSD S_Z of the input motion and the transfer functions G_i's on the RHS (right-hand-side) are unknown a priori. As discovered in [17], it is possible to eliminate these unknowns algebraically so that the noise PSD is expressed explicitly in terms of the auto and cross PSDs only:

$$S_{ei} = S_{ii} - S_{ji} \frac{S_{ik}}{S_{jk}} \tag{5}$$

In digital computation, the theoretical PSDs on the RHS in (5) are substituted by their sample estimates calculated from data, i.e.,

$$\hat{S}_{ei} = \hat{S}_{ii} - \hat{S}_{ji} \frac{\hat{S}_{ik}}{\hat{S}_{jk}} \tag{6}$$

where the hats on the PSDs on the RHS denote that they are sample estimates. To produce them, the data acquired from the sensor is first divided into non-overlapping segments of equal length. The sample PSD of each segment is then calculated and averaged. A more sophisticated means such as the Welch method is available [31], which allows segments to overlap and modulated by a non-rectangular window function.

In (5), theoretically the noise PSD S_{ei} is real-valued. However, this is not true when the theoretical PSDs are substituted by their sample counterparts because the sample estimates

need not obey (3)-(4). It can be verified that the value of S_{ei} in (5) will become its complex conjugate if j and k are swapped. This suggests that a legitimate way is to take only the real part of the RHS as the noise PSD estimate.

2.1 Bias due to misalignment

The three-channel method and hence (5) assumes that the three channels are oriented along exactly the same direction. In reality this is never the case, which leads to bias in the noise PSD estimate. In this section the problem is investigated analytically to yield an explicit expression for the bias due to misalignment. For this purpose the multi-dimensional nature of the input motion must be captured in the mathematical modelling.

Consider three collocated uni-directional sensors (say Sensors i, j and k) oriented along possibly different directions. Let the common input motion be varying in a d-dimensional space with components collected in a vector $\mathbf{z} = [z_1, ..., z_d]^T$ (omitting dependence on time for notational simplicity), where d can be 1, 2 or 3. Let Sensor i (say) be oriented with respect to the d axes with direction cosines collected in a vector $\mathbf{r}_i = [r_{i1}, ..., r_{id}]^T$. These are illustrated in Fig. 2 for $d = 2$. Clearly, the projection of input motion along Sensor i is $\mathbf{r}_i^T\mathbf{z}$. In the time domain, the output signal is given by

$$x_i = g_i * \left(\mathbf{r}_i^T\mathbf{z}\right) + n_i \tag{7}$$

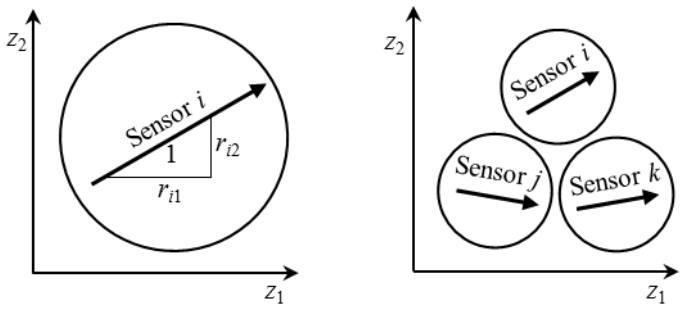

(a) Illustration of direction cosines (b) Sensor layout

Fig. 2 Schematic diagram for three sensors with possibly different orientations in the three-channel method

where g_i and n_i denote respectively the impulse response and channel noise as in (1). In the frequency domain, analogous to (2),

$$X_i = G_i \mathbf{r}_i^T \mathbf{Z} + \varepsilon_i \tag{8}$$

where **Z** is the scaled FT of **z**; G_i and ε_i are defined as before in (2). Similar expressions can be written for Sensors *j* and *k*. The auto PSD S_{ii} of X_i and cross PSD S_{ji} between Channels *j* and *i* (and hence S_{jk} and S_{ik}) are now given by

$$S_{ii} = G_i \mathbf{r}_i^T \mathbf{S}_Z \mathbf{r}_i \, G_i^* + S_{ei} \tag{9}$$

$$S_{ji} = G_j \mathbf{r}_j^T \mathbf{S}_Z \mathbf{r}_i \, G_i^* \quad S_{jk} = G_j \mathbf{r}_j^T \mathbf{S}_Z \mathbf{r}_k G_k^* \quad S_{ik} = G_i \mathbf{r}_i^T \mathbf{S}_Z \mathbf{r}_k G_k^* \tag{10}$$

where $\mathbf{S}_Z = E(\mathbf{Z}\mathbf{Z}^*)$ is the *d*-by-*d* PSD matrix of the *d*-dimensional input motion. Substituting the new expressions of PSDs in (9) and (10) into (5) as an estimation formula and then collecting terms, it can be shown algebraically that the fractional bias in the estimate of noise PSD is given by

$$e_i = \frac{\hat{S}_{ei} - S_{ei}}{S_{ei}} = \frac{G_i G_i^*}{S_{ei}} (\mathbf{r}_i^T \mathbf{S}_Z \mathbf{r}_i \; - \mathbf{r}_j^T \mathbf{S}_Z \mathbf{r}_i \; \frac{\mathbf{r}_i^T \mathbf{S}_Z \mathbf{r}_k}{\mathbf{r}_j^T \mathbf{S}_Z \mathbf{r}_k}) \tag{11}$$

where $\hat{S}_{ei}$ and S_{ei} denote respectively the sample estimate and theoretical (true) value of the noise PSD. In terms of PSD, the signal-to-noise ratio (SNR) of Sensor *i* is

$$\gamma_i = \frac{G_i G_i^* \mathbf{r}_i^T \mathbf{S}_Z \mathbf{r}_i}{S_{ei}} \tag{12}$$

Equation (11) can be now written in a more intuitive form as

$$e_i = \gamma_i (1 - \frac{c_{ji} c_{ik}}{c_{ii} c_{jk}}) \tag{13}$$

where

$$c_{ji} = \mathbf{r}_j^T \mathbf{S}_Z \mathbf{r}_i \tag{14}$$

is the cross PSD between Channels j and i; c_{ik}, c_{ii} and c_{jk} are defined similarly.

2.2 Applicability

Using (13), it can be verified that $e_i = 0$ if the three sensors have exactly the same orientation (i.e., $\mathbf{r}_i = \mathbf{r}_j = \mathbf{r}_k$), because then $c_{ji} = c_{ik} = c_{ii} = c_{jk}$. This checks with the context for which the three-channel method is applicable as conventionally understood. In the general case, the bias grows with the SNR γ_i but the extent depends on the direction cosines and the cross PSD of the input motions between sensors in a somewhat non-trivial manner. Based on (13), below are three special cases where the three-channel method is still applicable (i.e., bias identically or approximately zero) even when there is alignment error:

(i) Low SNR: this can be seen from (13) when γ_i is small and the parenthesis is O(1). Low SNR is often encountered at low frequencies, e.g., for 'pink' noise whose PSD is inversely proportional to frequency.

(ii) Unidirectional motion ($d = 1$): when $d = 1$, $\mathbf{S}_Z$ and the direction cosines ($\mathbf{r}_i$, $\mathbf{r}_j$, $\mathbf{r}_k$) in (13) are all scalars. The parenthesis (and hence the bias) then vanishes because the quotient inside is identically equal to 1:

$$\frac{c_{ji} c_{ik}}{c_{ii} c_{jk}} = \frac{r_j r_i^2 r_k S_Z^2}{r_j r_i^2 r_k S_Z^2} = 1 \tag{15}$$

Note that the direction of input motion can be arbitrary and need not coincide with the direction of any sensor. The discovery of this case and its generalisation leads to the new method in Section 3 later.

(iii) There is at least one sensor with the same orientation as the target sensor (i in (13)): this is a non-trivial and important case to note, which widens the scope of the three-channel method. To see this, suppose Sensor j has the same orientation as Sensor i, i.e., $\mathbf{r}_j = \mathbf{r}_i$. Then the parenthesis of (13) vanishes because $c_{ji} = c_{ii}$ and $c_{ik} = c_{jk}$; and the quotient inside is identically equal to 1 regardless of $\mathbf{r}_k$. Although the orientation of the third sensor (k here) does not affect the bias, it does increase the variance of the estimates. This will be demonstrated using synthetic data later in Fig. 5(b) in Section 2.3. Thus, despite this discovery, in practice all the three channels are still advised to be aligned as close as possible.

2.3 Numerical investigation

In this section, we investigate how alignment error and SNR influence the accuracy of the estimated noise PSD using synthetic data. Consider three collocated uniaxial sensors subjected to a common input motion within the x-y plane (i.e., z component = 0), as shown in Fig. 3. All the data channels are in the x-y plane. Sensor i is oriented at 10° anticlockwise from the global x-direction. Sensors j and k are oriented along a different but common direction, with an angle offset of θ further from Sensor i. The noise of all data channels and the (common) input motion are simulated to be independent white noise. The (one-sided) noise PSD of each channel is equal to 10^{-15} g^2/Hz. The data is generated based on (7) (taking g_i's as unit impulse for simplicity) with different PSD values of the input motion along the global x- and y-axis, which are denoted respectively by S_x and S_y. Three hours of data at 200 Hz is divided into 1080 non-

overlapping segments to produce the averaged sample PSD with a frequency interval of 0.1 Hz and a sample c.o.v. (coefficient of variation) of $1/\sqrt{1080} \approx 3\%$.

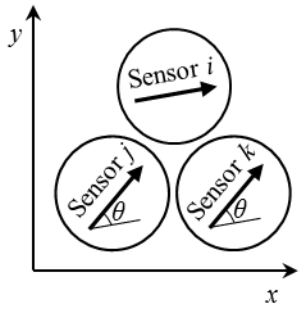

Fig. 3 Sensor layout, synthetic data, three-channel method

Consider $S_y = 1.5S_x$ so that the input motion is two-dimensional (d = 2). Fig. 4(a) shows the bias in the estimated noise PSD of Sensor i versus the SNR γ_i for different alignment errors (θ = 0°, 5° and 10°). Analogous to (11), the bias is quantified by $e_i = \left|\bar{S}_{ei} - S_{ei}\right| / \left|S_{ei}\right|$ where $S_{ei} = 10^{-15}$ g^2/Hz is the target value of the noise PSD and $\bar{S}_{ei}$ is the averaged value of estimated noise PSD over the frequency range 0.1-90 Hz. This definition of bias, averaging over frequencies rather than data sets, is convenient and legitimate for this example because the estimates at different frequencies are identically distributed; target spectrum is white. The frequency band has been chosen so that it starts with the lowest non-zero frequency (= 1/duration of window segment) and ends at a frequency away from the Nyquist frequency. The analytical results based on (13) (solid line) agree with the empirical values directly calculated from data (star and diamond). When the sensors are oriented along the same direction (i.e., θ = 0°), the bias is practically zero (to within statistical error due to finite number of averages) regardless of SNR, as expected. When there is alignment error (θ = 5° and 10°), the bias increases with SNR in a linear manner on a log-log plot. This can be reasoned from (13), where the parenthesis depends on correlations that remain the same and so the bias e_i increases linearly with SNR γ_i. Besides, the diamonds (θ = 10°) are above the stars (θ = 5°), i.e., the larger the alignment error, the

higher the bias. Fig. 4(b) shows the results when $S_y = 0$, i.e., the input motion is uni-directional ($d = 1$) along the x-axis. In this case the bias is practically zero (to within statistical error) regardless of SNR, which agrees with Point (ii) in Section 2.2. Note that the input motion is not along the direction of the Sensor i.

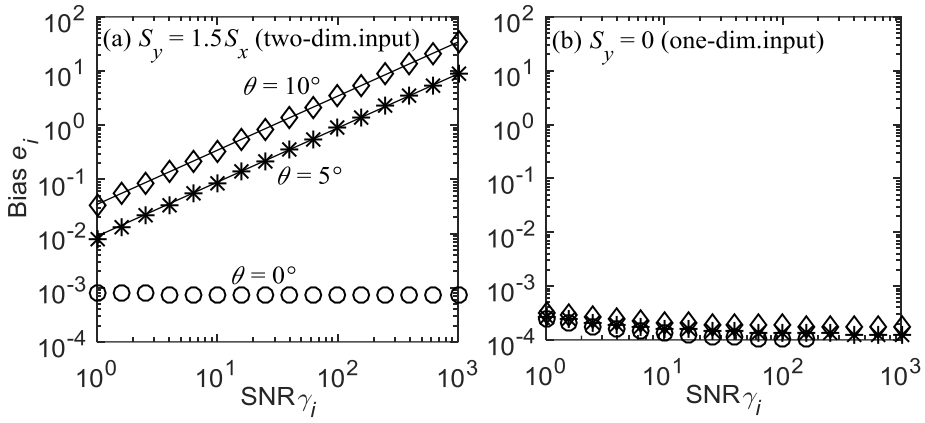

Fig. 4 Bias in the estimated noise PSD versus the SNR of Sensor i for different alignment errors. (a) $S_y = 1.5S_x$; (b) $S_y = 0$. Circle - $\theta = 0°$; star - $\theta = 5°$; diamond - $\theta = 10°$; solid line - analytical result using (13)

According to Point (iii) in Section 2.2, the three-channel method is unbiased when there is at least one another channel with the same orientation. This is illustrated in Fig. 5(a), which shows that the bias is practically zero (to within statistical error) regardless of SNR when Sensors i and j have the same orientation (at 10º from the x-axis) and Sensor k has different orientations of $\theta = 0°$, 10°, 30° and 60° further from Sensor i . Fig. 5(b) shows the sample c.o.v. of the noise PSD estimate, which increases with the SNR and θ. This shows that even though the orientation of Sensor k does not affect the unbiased nature of Sensor i, its alignment deviation does reduce the statistical accuracy of the noise PSD estimate.

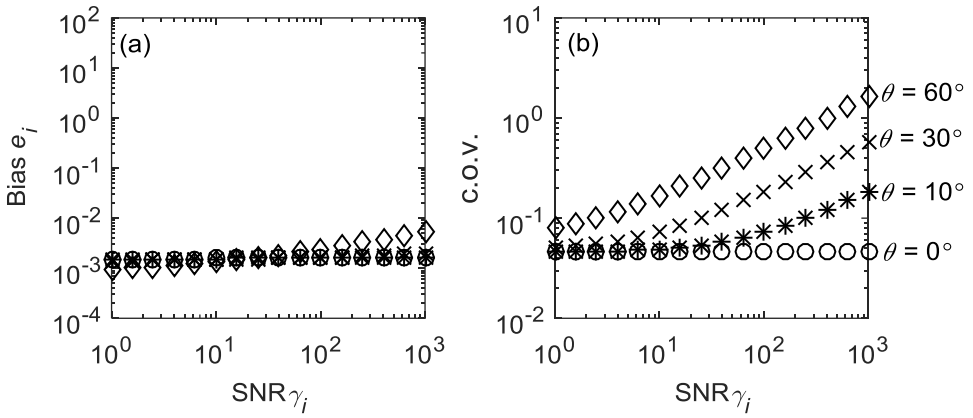

Fig. 5 Bias and sample c.o.v. in the estimated noise PSD versus SNR of Sensor *i* when Sensor *j* has the same orientation but Sensor *k* has an angle offset of θ. (a) Bias versus SNR; (b) sample c.o.v. versus SNR. Circle - θ = 0°; star - θ = 10°; cross - θ = 30°; diamond - θ = 60°

2.4 Experimental investigation

As mentioned in Point (iii) of Section 2.2, the noise PSD of Channel *i* is still unbiased if there is at least one channel with the same orientation. This aspect is further illustrated in this section through an experiment where the orientations of the sensors have been specially planned for this purpose. Fig. 6(a) shows a general view of the experiment performed under laboratory environment. Although the three-channel method requires only three sensors, five sensors are used in the experiment for scientific investigation so that different sets of data can be obtained under different configurations but under the same time period. Two sets of experiments have been carried out with five triaxial servo-accelerometers, i.e., A to E indicated in the figure. In the first setup shown in Fig. 6(b), E, C and D have the same orientation (to within practical precision) while A and B are oriented along a different but common direction. The angle between these two groups of sensors is 60°. In the second setup shown in Fig. 6(c), A is oriented differently with a clockwise angle offset of 15° compared to that in the first setup. Triaxial data for all the sensors was recorded at 200 Hz for 3 hours in each setup. It was then divided into 1080 non-overlapping segments to produce the averaged sample PSD. The investigation here will focus on estimating the noise PSD of the North channel (parallel to the handle) of E.

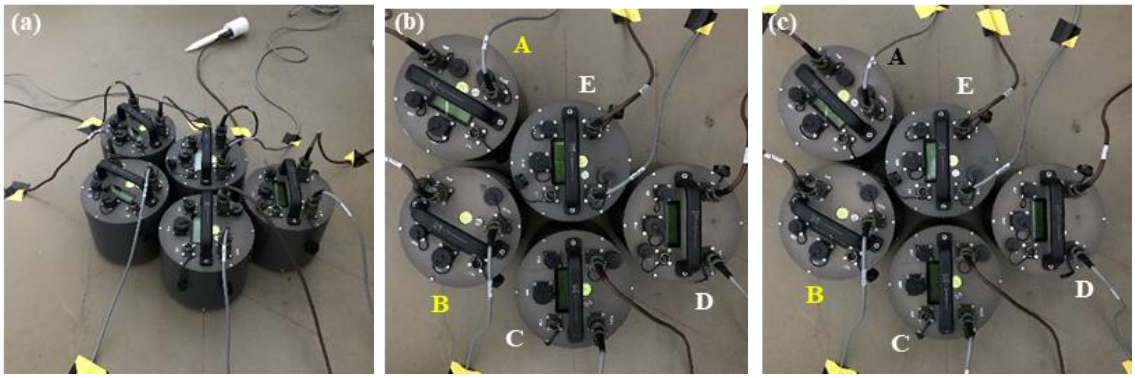

Fig. 6 Experimental setup. (a) General view; (b) Setup 1; (c) Setup 2

Sensors C, D and E are oriented along the same direction and so the three-channel method is applicable to determining their noise PSDs as conventionally understood. Note that only the North channel data of the sensors is needed to produce the results of the three-channel method. Inevitably, the sensors are placed at distinct locations, which violates the assumption of collocated channels and hence leads to modelling error in the results. In view of this, the sensors are deliberately placed as close as possible, forming an equilateral triangle so that spatial incoherence has a similar effect on different pairs of channels. The results are summarised in Fig. 7 and discussed as follow.

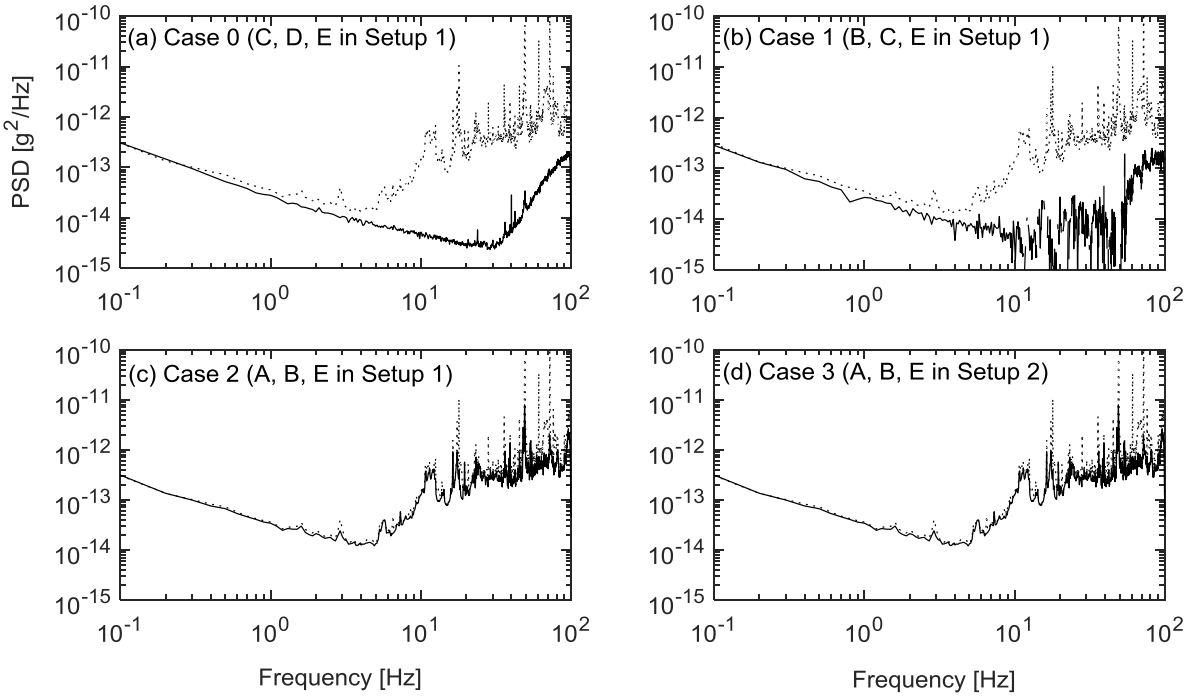

Fig. 7 Data PSD (dotted line) and noise PSD (solid line) of the North channel of Sensor E estimated by the three-channel method

Case 0 (C, D, E in Setup 1): Fig. 7(a) shows the estimated noise PSD of the North channel of Sensor E based on the data of C, D and E in the first setup. The PSD of the data itself (noise + vibration) is also plotted to give an idea of the SNR. It can be seen that the noise PSD shows a linearly decreasing trend below 20 Hz on a log-log plot and the slope is about 1, revealing a 1/f type of noise (i.e., pink noise) dominating in this band. Beyond 30 Hz, the noise PSD estimate increases with frequency. The results for C and D are similar and they are not shown here.

Case 1 (B, C, E in Setup 1): Fig. 7(b) shows the results when the data of B, C and E are used for estimating the noise PSD of E. This corresponds to the case described in Point (iii) of the Section 2.2 when only one another sensor has the same orientation as the target sensor. Except for moderately high frequencies (say > 5 Hz), the estimated noise PSD agrees well with that shown in Fig. 7(a), which demonstrates the point that the three-channel method is still applicable. This does not appear to be so beyond 5 Hz (say), however. This can be explained based on the finding in Fig. 5(b). Essentially, while the noise PSD of E is still unbiased

regardless of the orientation of B, its variance is larger than that when B is along the same direction. The variance also increases with the SNR. The discrepancy between the noise PSD estimate in Fig. 7(b) from its 'benchmark value' in Fig. 7(a) is therefore of statistical error nature, which can be reduced by using longer data length.

Case 2 (A, B, E in Setup 1): Fig. 7(c) shows the results when the data of A, B and E in Setup 1 are used to estimate the noise PSD of E. Despite the fact that A and B are oriented along the same direction, the noise PSD estimate of E is significantly biased (high in this case) because E is oriented differently. This again demonstrates Point (iii) in Section 2.2. This is also true when A, B and E are all oriented differently in Case 3, as shown in Fig. 7(d).

It is seen from Fig. 7(a)-(d) that the data PSD almost overlaps with the noise PSD below 2 Hz. This demonstrates Point (i) of Section 2.2 regarding low SNR. The different cases discussed here are summarised in Table 1.

Table 1 Summary of the cases discussed in Section 2.4

Case	Data	Remark
0	C, D, E in Setup 1	All sensors have the same orientation. The three-channel method works (unbiased) as conventionally understood.
1	B, C, E in Setup 1	Only one sensor (C) has the same orientation as the target (E). The three-channel method works (unbiased) as discovered in this work. However, the c.o.v. of estimate increases with SNR; see Fig. 5(b).
2	A, B, E in Setup 1	No sensor has the same orientation as the target (E). The three-channel method does not work (biased), despite two sensors (A & B) have the same orientation.
3	A, B, E in Setup 2	No sensor has the same orientation as the target (E). The three-channel method does not work (biased).

3. Three-Sensor method

The investigation in Section 2 reveals explicitly the role of alignment error and SNR on the bias in the three-channel method. Leveraging on such understanding, in this section a new

method is developed that is unbiased regardless of sensor orientations, thereby significantly enhancing the robustness and accuracy of the calibration procedure.

3.1 Modelling of input motion and data

Consider three collocated sensors (say Sensors *i*, *j* and *k*) with possibly different orientations but subjected to a common input motion. Each sensor can measure *d* directions (*d* = 1, 2 or 3). In the three-channel method, the three data channels for estimating the noise PSD were assumed to measure exactly the same, i.e., one-dimensional projection of the input motion. Investigation on the mathematical structure of the calibration problem (e.g., Section 2.1) reveals that the alignment-induced bias of the three-channel method stems from the lower (one) dimension of the modelled motion compared to the actual input motion (*d* here). In view of this, as the key of the proposed method, the modelled input motion is assumed to be fully *d*-dimensional, collected in a vector $\mathbf{z} = [z_1, ..., z_d]^T$. Let the output signal measured by the *d* channels of Sensor *i* (say) be collected in a vector $\mathbf{x}_i = [x_{i1}, ..., x_{id}]^T$. Let $\mathbf{R}_i$ be a *d*-by-*d* 'projection matrix' of Sensor *i*. It projects the input motion ($\mathbf{z}$) in global coordinate system onto the space (of the same dimension) spanned and measured by the channels of Sensor *i* (in local coordinate system), which is equal to $\mathbf{R}_i\mathbf{z}$. Note that the *d* channels of the sensor need not be orthogonal, but they need to span a *d*-dimensional space so that $\mathbf{R}_i$ is square and invertible. Although the channels of multi-axial sensors are typically orthogonal, having the theory not requiring them to be so allows for more robustness. This is relevant, e.g., when biaxial (or triaxial) sensors are made up of uniaxial sensors arranged in-house. The essential requirement is that the dimension of the space spanned by the input motion, i.e., the 'input space', is preserved when it is projected onto the space spanned by the channels of each sensor, i.e., the 'sensor space'. The input space and the sensor space need not be the same, however. Geometrically, the (*r*, *s*)-entry of $\mathbf{R}_i$ is equal to the cosine of the angle between the direction of

Channel r and z_s. It should be noted that the expression of $\mathbf{R}_i$ is not needed in the proposed method but it is explained here for clarity. In the above context, the output signal of Sensor i in the time domain is given by

$$\mathbf{x}_i = \mathbf{g}_i * (\mathbf{R}_i \mathbf{z}) + \mathbf{n}_i \tag{16}$$

where $\mathbf{g}_i$ is a d-dimensional diagonal matrix containing the impulse responses of the channels of Sensor i; $\mathbf{n}_i$ is a d-by-1vector containing the noise of the data channels of Sensor i. In the frequency domain, the relationship analogous to (16) is

$$\mathbf{X}_i = \mathbf{G}_i \mathbf{R}_i \mathbf{Z} + \boldsymbol{\varepsilon}_i \tag{17}$$

where $\mathbf{X}_i$, $\mathbf{G}_i$, $\mathbf{Z}$ and $\boldsymbol{\varepsilon}_i$ denote respectively the scaled FTs of $\mathbf{x}_i$, $\mathbf{g}_i$, $\mathbf{z}$ and $\mathbf{n}_i$.

Similar to the three-channel method, the noise of different channels are assumed to be uncorrelated and they are also uncorrelated from the input motion. The unknown transfer function $\mathbf{G}_i$ and projection matrix $\mathbf{R}_i$ in (17) can be combined into a single matrix by defining

$$\mathbf{H}_i = \mathbf{G}_i \mathbf{R}_i \tag{18}$$

Note that $\mathbf{H}_i$ is invertible because $\mathbf{G}_i$ and $\mathbf{R}_i$ are. The auto PSD and cross PSD matrices related to Sensor i are then given by

$$\mathbf{S}_{ii} = \mathbf{H}_i \mathbf{S}_Z \mathbf{H}_i^* + \mathbf{S}_{ei} \tag{19}$$

$$\mathbf{S}_{ji} = \mathbf{H}_j \mathbf{S}_Z \mathbf{H}_i^* \quad \mathbf{S}_{jk} = \mathbf{H}_j \mathbf{S}_Z \mathbf{H}_k^* \quad \mathbf{S}_{ik} = \mathbf{H}_i \mathbf{S}_Z \mathbf{H}_k^* \tag{20}$$

where $\mathbf{S}_{ji} = E(\mathbf{X}_j \mathbf{X}_i^*)$ denotes the cross PSD matrix between Sensors j and i; similar notations apply to other matrices; $\mathbf{S}_Z = E(\mathbf{Z}\mathbf{Z}^*)$ denotes the PSD matrix of the input motion; $\mathbf{S}_{ei} = E(\mathbf{n}_i \mathbf{n}_i^*)$ denotes the noise PSD matrix of Sensor i.

3.2 Estimation formula

In (19)-(20), the target is to find the noise PSD matrix $\mathbf{S}_{ei}$. The auto/cross PSD matrices (e.g., $\mathbf{S}_{ji}$) can be estimated from data but the matrices $\mathbf{S}_Z$ and $\mathbf{H}_i$'s are not known a priori. Approaching the problem as solving simultaneous algebraic scalar equations arising from the matrix entries turns out to be intractable, especially that the entries are generally complex-valued and the matrices have special structure (e.g., Hermitian). Fortunately, it has been discovered that the noise PSD matrices can in fact be solved algebraically in a manner analogous to the three-channel method.

First note from (19) that $\mathbf{S}_{ei} = \mathbf{S}_{ii} - \mathbf{H}_i \mathbf{S}_Z \mathbf{H}_i^*$. This suggests one to express $\mathbf{H}_i \mathbf{S}_Z \mathbf{H}_i^*$ in terms of the auto/cross PSD matrices of data, which turns out to be possible. This is derived as follow.

Post-multiplying the third equation in (20) by $(\mathbf{H}_k^*)^{-1}\mathbf{H}_i^*$ and swapping the LHS and RHS gives

$$\mathbf{H}_i \mathbf{S}_Z \mathbf{H}_i^* = \mathbf{S}_{ik} (\mathbf{H}_k^*)^{-1} \mathbf{H}_i^* \tag{21}$$

Pre-multiplying the second equation in (20) by $\mathbf{S}_{jk}^{-1}$ and post-multiplying by $(\mathbf{H}_k^*)^{-1}$ gives

$$(\mathbf{H}_k^*)^{-1} = \mathbf{S}_{jk}^{-1} \mathbf{H}_j \mathbf{S}_Z \tag{22}$$

Substituting (22) into (21) gives

$$\mathbf{H}_i \mathbf{S}_Z \mathbf{H}_i^* = \mathbf{S}_{ik} \mathbf{S}_{jk}^{-1} \mathbf{H}_j \mathbf{S}_Z \mathbf{H}_i^* \tag{23}$$

From the first equation in (20), $\mathbf{H}_j \mathbf{S}_Z \mathbf{H}_i^* = \mathbf{S}_{ji}$, and so

$$\mathbf{H}_i \mathbf{S}_Z \mathbf{H}_i^* = \mathbf{S}_{ik} \mathbf{S}_{jk}^{-1} \mathbf{S}_{ji} \tag{24}$$

Substituting (24) into (19), the noise PSD $\mathbf{S}_{ei}$ of Sensor *i* is therefore given by

$$\mathbf{S}_{ei} = \mathbf{S}_{ii} - \mathbf{S}_{ik}\mathbf{S}_{jk}^{-1}\mathbf{S}_{ji} \tag{25}$$

This expression is analogous to (5) except that the terms are now all *d*-by-*d* matrices, where *d* is the dimension of the input motion. When $d = 1$, (25) reduces to (5), i.e., the three-channel method is a special case of the proposed method.

Equation (25) is remarkably simple, although the original problem is algebraically non-trivial. The simple formula here stems from the discovery of the algebraic structure of the cross PSD matrices among three sensors when the dimension of the measured channels matches the dimension of the input motion.

Technically, the derivation of (25) (hence the method) requires $\mathbf{H}_k$ and $\mathbf{S}_{jk}$ to be invertible. The former is guaranteed by the $\mathbf{R}_i$'s being invertible. The latter essentially requires that the other two sensors *j* and *k* need to contain some common influence from the unknown input so that it can be removed when $\mathbf{S}_{jk}^{-1}$ is multiplied with $\mathbf{S}_{ik}$ and $\mathbf{S}_{ji}$. Since $\mathbf{S}_{jk} = \mathbf{H}_j\mathbf{S}_Z\mathbf{H}_k^*$, it can be seen that $\mathbf{S}_{jk}$ (and hence $\mathbf{S}_{ji}$ and $\mathbf{S}_{ik}$) is invertible if and only if $\mathbf{S}_Z$ is invertible.

In the proposed method, sensor orientations are irrelevant to the bias of the estimated noise PSD, which significantly improves the robustness and accuracy of huddle test. Since the projection matrices are not explicitly involved, the *d*-components measured by each sensor do not need to be perpendicular. As the proposed method is based on three collocated sensors, it is named as 'three-sensor method'.

Theoretically, when (19)-(20) hold, $\mathbf{S}_{ei}$ in (25) is a real diagonal matrix and can be shown to remain the same when *j* and *k* are swapped. However, this is not necessarily true in implementation when the PSD matrices are replaced by their sample counterparts estimated from data, for the same reason in the three-channel method. By a similar reasoning in (6), the

following is a legitimate estimation formula that always returns real values in the diagonal entries:

$$\hat{\mathbf{S}}_{ei} = \hat{\mathbf{S}}_{ii} - (\hat{\mathbf{S}}_{ik}\hat{\mathbf{S}}_{jk}^{-1}\hat{\mathbf{S}}_{ji} + \hat{\mathbf{S}}_{ij}\hat{\mathbf{S}}_{kj}^{-1}\hat{\mathbf{S}}_{ki})/2 \tag{26}$$

where the hat denotes that the quantity is a sample estimate calculated from data.

3.3 Numerical investigation

In this section, the proposed method is verified using synthetic data generated based on (16) (taking $\mathbf{g}_i$'s as the identity matrix for simplicity). Consider three collocated biaxial sensors subjected to a common input motion. All the data channels are in the *x*-*y* plane and $d = 2$. The sensor layout is shown in Fig. 8. Channel 1 of Sensor *i* is oriented along the global *x*-axis. Channels 1 of Sensors *j* and *k* are oriented with an angle offset of θ with Channel 1 of Sensor *i*. The two channels of each sensor are not perpendicular and the angle between them is indicated in Fig. 8. The input motion has independent white noise components along the *x*- and *y*-directions with PSD S_x (to be varied) and $S_y = 1.5S_x$, respectively. The noise of all data channels are assumed to be white with a PSD of 10^{-15} g^2/Hz. Biaxial (Channels 1 and 2 of each sensor) data is recorded for three hours at 200 Hz. It is then divided into 1080 non-overlapping segments to produce the averaged sample PSD.

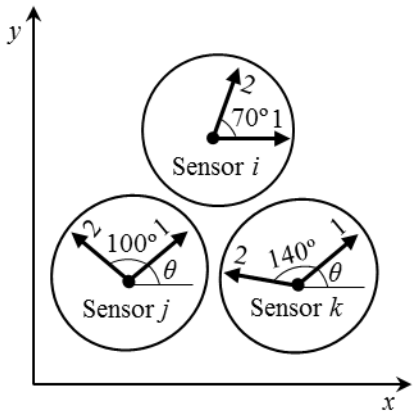

Fig. 8 Sensor layout, synthetic data, three-sensor method

Consider estimating the noise PSD of Channel 1 of Sensor *i*. Fig. 9 shows the bias calculated from data versus SNR for different alignment errors (θ = 0°, 5° and 10°). As the noise PSD is fixed, the SNR is varied by changing the PSD of the input motion. The bias is defined as in Section 2.3 in an average sense over the frequency range 0.1-90 Hz. When Channel 1 of the sensors are oriented along the same direction (θ = 0°), the bias for both the three-channel method (circle, using Channel 1 of sensors) and the proposed method (star, using Channels 1 & 2 of sensors) is practically zero (to within statistical error). When there is alignment error (θ = 5° and 10°), the bias of the three-channel method increases with SNR and alignment error (as already illustrated in Section 2.3) but the bias for the proposed method is still practically zero regardless of SNR and orientations.

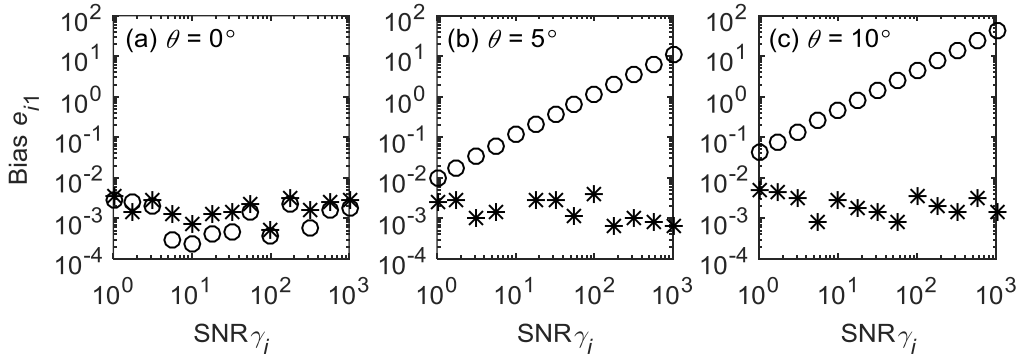

Fig. 9 Bias in the estimated noise PSD versus the SNR of Channel 1 of Sensor *i* for different sensor orientations. (a) θ = 0°; (b) θ = 5°; (c) θ = 10°. Circle - three-channel method; star - proposed method

3.4 Experimental investigation

In this section, the proposed method is investigated using the same data and experimental cases in Section 2.4; see also Table 1. The results are shown in Fig. 10, where the results from the three-channel method presented before in Fig. 7 are also plotted (in solid black line) for comparison.

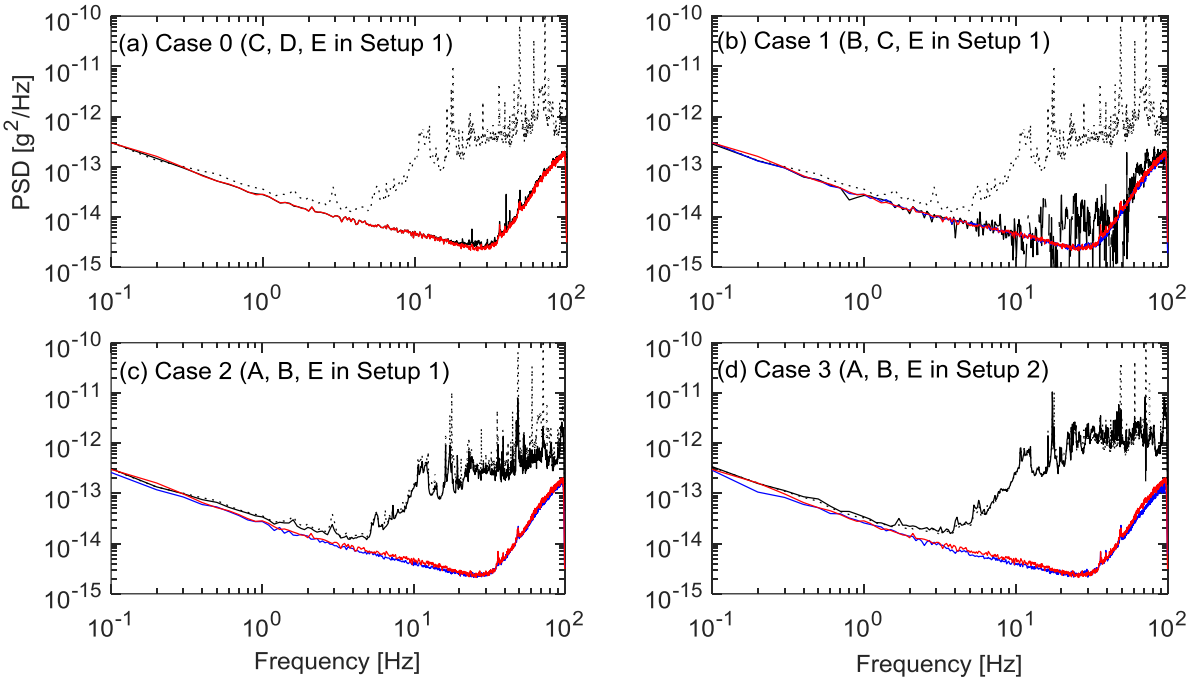

Fig. 10 Data PSD (dotted black line) and noise PSD of the North channel of Sensor E estimated by the three-channel method (solid black line) and the proposed method (red line in (a) and blue line in (b) - (d)) using experimental data; red line in (b)-(d): benchmark of the noise PSD estimate copied from the red line in (a)

Fig. 10(a) shows that when the data of C, D and E are used, the noise PSD of Sensor E calculated by both methods practically coincide. As there is no 'exact' value of the noise PSD, the noise PSD in Fig. 10(a) (the best possible situation) is used as the benchmark for comparison in other cases. In Fig. 10(b)-(d), the noise PSD estimate of the proposed method (blue line) visually coincides with the benchmark value (red line). In particular, Fig. 10(d) demonstrates that the method remains unbiased in the general situation when all the sensors have arbitrary and possibly different orientations.

3.5 Effect of angle between channels of a sensor

As mentioned in Section 3.2, the proposed method is applicable (i.e., unbiased) regardless of the angles between the multi-axial channels of a sensor, as long as they span a space of dimension equal to that of the input motion and the dimension of the input space is preserved in the projection onto the sensor space. Nevertheless, numerical experiments reveal that the

c.o.v. tends to increase when the angle decreases from 90º, i.e., as the channels become more 'collinear', which is intuitive. This is illustrated by a numerical experiment as follow.

Consider three collocated biaxial sensors measuring a common input motion within the *x*-*y* plane, as shown in Fig. 11. Channel 1 of Sensor *i* is oriented along the global *x*-axis. Channels 1 of Sensors *j* and *k* are oriented with an angle offset of θ with Channel 1 of Sensor *i*. The angle between the biaxial channels of each sensor, i.e., the 'channel angle', is denoted by α. Similar to Section 3.3, the input motion has independent white noise components along the *x*- and *y*-directions with PSD S_x (to be varied) and $S_y = 1.5S_x$, respectively. The noise of all data channels are white with a PSD of 10^{-15} g^2/Hz. Ten hours of biaxial data at 200 Hz is recorded and then divided into 3600 non-overlapping segments to produce the averaged sample PSD.

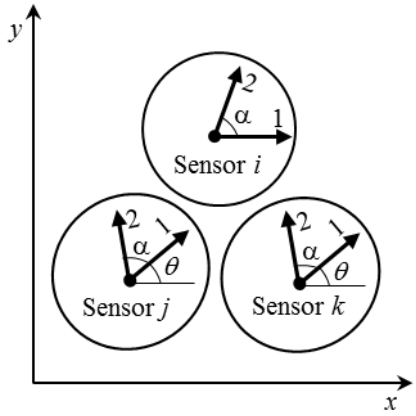

Fig. 11 Sensor layout, synthetic data, effect of the 'channel angle'

Consider θ = 5º. Fig. 12(a) shows the bias (as defined in Section 2.3) in the estimated noise PSD of Channel 1 of Sensor *i* versus α for SNR = 10, 100 and 1000. It can be seen that the noise PSD estimates are unbiased regardless of channel angle and SNR. Fig. 12(b) shows the sample c.o.v. of the noise PSD estimate. It decreases with the channel angle and reaches a minimum when α = 90º , i.e., the biaxial channels are perpendicular. The circles (SNR = 10), stars (SNR = 100) and diamonds (SNR = 1000) are almost overlap, i.e., the c.o.v. is insensitive to SNR.

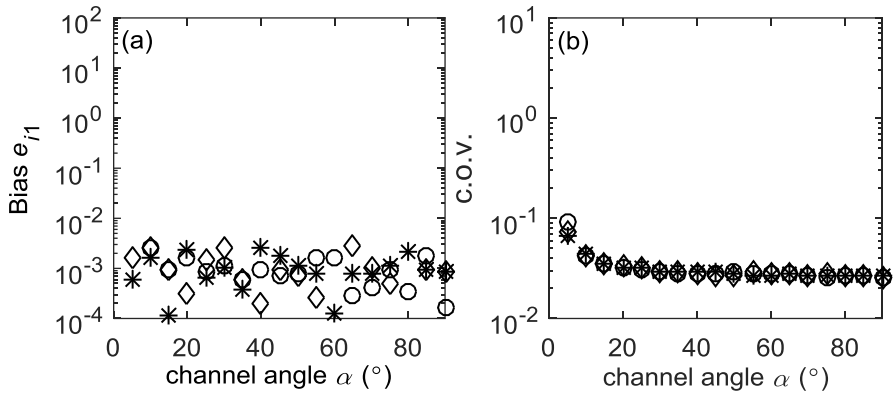

Fig. 12 Bias and sample c.o.v. in the estimated noise PSD of Channel 1 of Sensor *i* versus the 'channel angle' α, i.e., the angle between the biaxial channels of Sensor *i*, when θ = 5º. (a) Bias versus α; (b) sample c.o.v. versus α. Circle - SNR = 10; star - SNR = 100; diamond - SNR = 1000

Consider SNR = 100. Fig. 13 shows the results analogous to Fig. 12 but now for different alignment errors (θ = 5º, 20º, 45º and 60º). Fig. 13(a) shows that the bias is practically zero (to within statistical error) regardless of alignment error and channel angle. From Fig. 13(b), the c.o.v. tends to be bigger with smaller channel angle and larger alignment error. It reaches the same minimum (to within statistical error) regardless of alignment error when α = 90º, i.e., the alignment error does not affect statistical accuracy when the sensors have orthogonal channels. In view of this, even though the proposed method is unbiased regardless of the channel angle, the channels of each sensor are still recommended to be perpendicular or as much as possible when constraint permits.

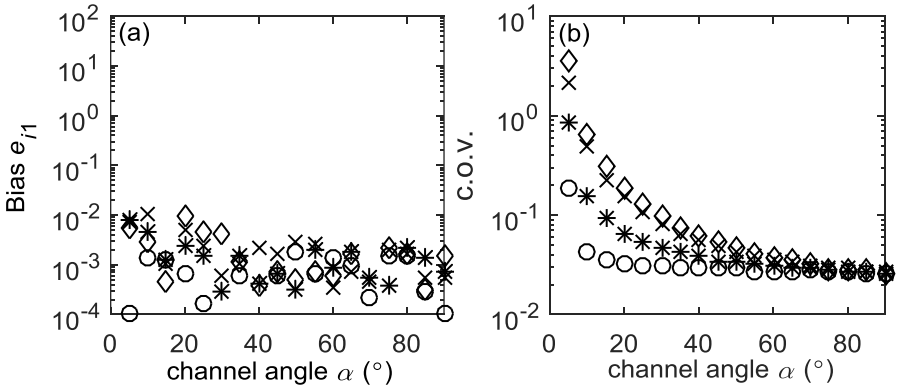

Fig. 13 Bias and sample c.o.v. in the estimated noise PSD of Channel 1 of Sensor *i* versus the 'channel angle' α, i.e., the angle between the biaxial channels of Sensor *i*, when SNR = 100. (a) Bias versus α; (b) sample c.o.v. versus α. Circle - θ = 5º; star - θ = 20º; cross - θ = 45º; diamond - θ = 60º

4. Effect of spatial incoherence

For both the three-channel method and the proposed method, one basic but pivotal assumption is that the three sensors are subjected to a common input motion, i.e., they are spatially perfectly coherent. In implementation, this assumption can be violated, leading to bias in the estimated noise PSD. This issue is investigated in this section.

4.1 Bias due to misalignment and spatial incoherence

First consider the three-channel method. When the motions at different sensors are not perfectly coherent, the data of Sensor *i* in (8) should be modelled (in the frequency domain) as

$$X_i = G_i \mathbf{r}_i^T \mathbf{Z}_i + \varepsilon_i \tag{27}$$

where the one-dimensional projection of input motion, $\mathbf{r}_i^T \mathbf{Z}_i$, now depends on Sensor *i*. Following a similar derivation in Section 2.1, it can be shown that the bias is still given by (13) but now with incoherent motions $\mathbf{S}_Z$ in (12) should be replaced by $\mathbf{S}_{\mathbf{Z}_i\mathbf{Z}_i} = E(\mathbf{Z}_i\mathbf{Z}_i^*)$ and $\mathbf{S}_Z$ in (14) by $\mathbf{S}_{\mathbf{Z}_j\mathbf{Z}_i} = E(\mathbf{Z}_j\mathbf{Z}_i^*)$ (cross PSD matrix between input motions at Sensors *j* and *i*). In this case, one can deduce that for imperfect coherence Point (i) in Section 2.2 is still valid but Points (ii) and (iii) are not.

For the (proposed) three-sensor method, the data in (17) now reads

$$\mathbf{X}_i = \mathbf{G}_i \mathbf{R}_i \mathbf{Z}_i + \boldsymbol{\varepsilon}_i \tag{28}$$

where the *d*-dimensional input motion depends on the Sensor *i*. Equations (19)-(20) still holds except that $\mathbf{S}_Z$ should be replaced by the cross PSD matrix of input motions between the subject sensors, e.g., $\mathbf{S}_Z$ in the first equation of (20) should be replaced by $\mathbf{S}_{\mathbf{Z}_j\mathbf{Z}_i}$. Substituting the new versions of (19)-(20) into (25) as an estimation formula and simplifying gives

$$\hat{\mathbf{S}}_{ei} - \mathbf{S}_{ei} = \mathbf{H}_i \mathbf{S}_{\mathbf{Z}_i\mathbf{Z}_i} \mathbf{H}_i^* - \mathbf{H}_i \mathbf{S}_{\mathbf{Z}_i\mathbf{Z}_k} \mathbf{S}_{\mathbf{Z}_j\mathbf{Z}_k}^{-1} \mathbf{S}_{\mathbf{Z}_j\mathbf{Z}_i} \mathbf{H}_i^* \tag{29}$$

where $\hat{\mathbf{S}}_{ei}$ and $\mathbf{S}_{ei}$ are respectively the estimated and theoretical noise PSD. Pre-multiplying (29) with $\mathbf{S}_{ei}^{-1}$ and rearranging gives the bias as

$$\mathbf{e}_i = \mathbf{S}_{ei}^{-1}(\hat{\mathbf{S}}_{ei} - \mathbf{S}_{ei}) = \boldsymbol{\gamma}_i \left[\mathbf{I} - \left(\mathbf{H}_i^*\right)^{-1} \mathbf{S}_{\mathbf{Z}_i\mathbf{Z}_i}^{-1} \mathbf{S}_{\mathbf{Z}_i\mathbf{Z}_k} \mathbf{S}_{\mathbf{Z}_j\mathbf{Z}_k}^{-1} \mathbf{S}_{\mathbf{Z}_j\mathbf{Z}_i} \mathbf{H}_i^* \right] \tag{30}$$

where **I** is the identity matrix and

$$\boldsymbol{\gamma}_i = \mathbf{S}_{ei}^{-1}(\mathbf{H}_i \mathbf{S}_{\mathbf{Z}_i\mathbf{Z}_i} \mathbf{H}_i^*) \tag{31}$$

reflects the SNR in a generalised sense. Since $\mathbf{S}_{ei}$ is a diagonal matrix, the diagonal entries in $\mathbf{e}_i$ and $\boldsymbol{\gamma}_i$ are respectively the (fractional) bias and SNR of the data channels of Sensor *i*.

When the sensors are perfectly coherent, $\mathbf{e}_i = \mathbf{0}$ (i.e., unbiased, as expected) because then $\mathbf{S}_{\mathbf{Z}_i\mathbf{Z}_i} = \mathbf{S}_{\mathbf{Z}_i\mathbf{Z}_k} = \mathbf{S}_{\mathbf{Z}_j\mathbf{Z}_k} = \mathbf{S}_{\mathbf{Z}_j\mathbf{Z}_i}$ in (30). In fact, the estimate is unbiased as long as there is at least one (rather than two) another sensor (*j* or *k*) whose input is perfectly coherent with that of the target sensor (*i*). To see this, the bracket in (30) is zero when $\mathbf{Z}_j \equiv \mathbf{Z}_i$ or $\mathbf{Z}_k \equiv \mathbf{Z}_i$. This case is analogous to Point (iii) of Section 2.2, revealing that the proposed method is more robust with respect to spatial incoherence than is normally expected. In the general case when the sensors are spatially incoherent, the bias grows with the SNR but the extent depends on sensor orientations (through $\mathbf{H}_i^*$) and the cross PSD matrices of input motions between the sensors in a non-trivial manner, which will be investigated in the next section.

4.2 Experimental investigation

Recall the experimental setup in Fig. 6, where four cases were considered (see Table 1) and the sensors in each case were placed as close as possible in a form of an equilateral triangle. To

illustrate the effect of spatial incoherence, here we use the data from Sensors A, C and E to estimate the noise PSD of the North channel of E. Although A and C are both at equal (closest) distance from E (the target), they are separated further apart and hence have a lower coherence. Fig. 14(a) shows the results by the proposed method, analogous to Fig. 10. The results for the three-channel method are qualitatively similar to the black solid line in Fig. 7(b) (with larger fluctuations) and are omitted to simplify the picture. Compared to Fig. 10, there is now a significantly larger discrepancy between the estimated noise PSD (blue) and the benchmark value (red, copied from Fig. 10(a)) in the range (say) 20-50 Hz. This is likely to be due to lower coherence between A and C, which is also amplified by SNR. For the same reason, this is also true when the data of A, D and E are used, as evidenced in Fig. 14(b).

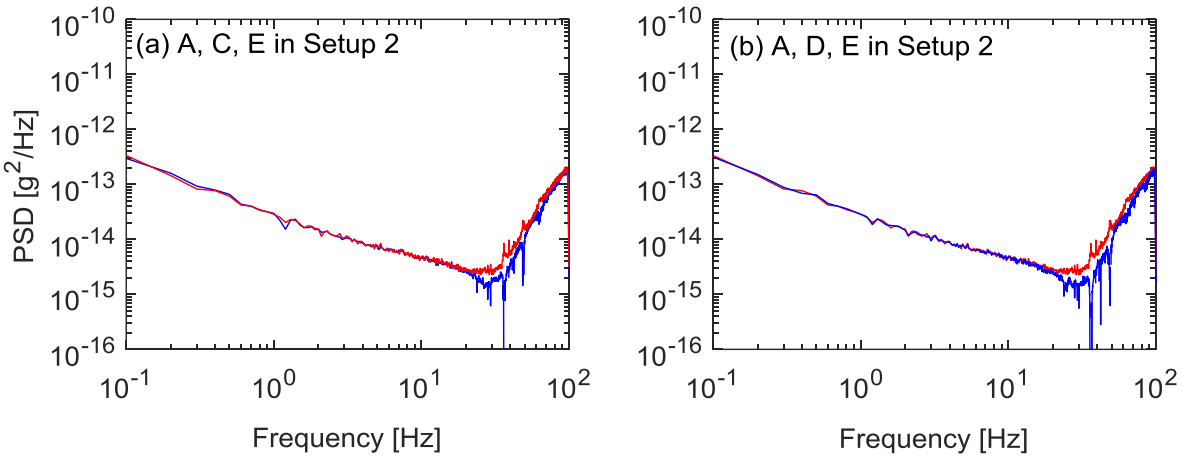

Fig. 14 Noise PSD of the North channel of E estimated by the proposed method (blue line); red line - benchmark value copied from the red line in Fig. 10(a)

5. Recommendations for the three-sensor method

Recommendations are in order when applying the proposed method. Put the sensors as close as possible to maximise coherence. Even though the proposed method is unbiased regardless of sensor orientations, it is still advised to align the sensors as closely as possible along the same direction as this can improve statistical accuracy. For the same reason, the multi-axial channels of each sensor are recommended to be mutually orthogonal or as much as possible

when constraint permits. Since the input motion is at most three-dimensional, using triaxial data can eliminate bias due to sensor orientations; that is, there is no restriction when using triaxial sensors. Bias can still be eliminated with lower dimensional (i.e., biaxial or uniaxial) data if the input motion is of a correspondingly lower dimension. Otherwise the sensor spaces of different sensors need to be the same, which requires precise alignment along some subset of directions. This is so that the motions measured by different sensors can still be fully accounted by a common (lower-dimensional) projection of the input motion on the common sensor space (and the theory in Section 3 applies).

As an example, suppose the input motion is three-dimensional. Calibrating using uniaxial data, e.g., the North channels of three sensors, will require the North channels to be precisely oriented so that the sensor spaces are all the same, being the one-dimensional space along the North direction. This corresponds to the three-channel method. Calibrating using biaxial data, say, the North and East channels, will require the (local) vertical channels to be precisely oriented along the same direction so that sensor spaces are all the same, being the two-dimensional space perpendicular to the vertical channels.

6. Conclusions

This work has provided a fundamental understanding on the bias in a huddle test and delivered a new method that allows instrument noise to be calibrated in a robust manner with no restrictions on sensor orientations. The bias due to misalignment stems from sensor channels spanning a space (i.e., the sensor space) of lower dimension than the input motion (i.e., the input space). Explicit formulas for the statistical bias of the three-channel method and the new method have been derived; see (13) and (30). The bias formula for the three-channel method clarifies the role and effect of alignment error; and discovers expanded scopes of applicability, i.e., when the input motion is one-dimensional or where only one (rather than two) another

sensor is required to have the same orientation as the target sensor. Matching the dimension of the sensor space and input space is the key to eliminating alignment-related bias, making the proposed method applicable for arbitrary sensor orientations. Inevitably, the proposed method still assumes perfect coherence among different sensors. The bias otherwise can be quantified by (30). The analytical findings and the proposed method have been verified by a series of investigations based on synthetic and experimental data.

7. Data and resources

All synthetic and experimental data in this work were obtained in the System Identification Laboratory at the University of Liverpool. They are available upon request by writing to zhuzuo@liverpool.ac.uk.

8. Acknowledgements

This work was funded by the UK Engineering & Physical Sciences Research Council (EP/N017897/1). The first author is supported by the Joint University of Liverpool/China Scholarship Council Scholarship. The third author is supported by tuition fellowship by the School of Engineering at the University of Liverpool. These financial supports are gratefully acknowledged.

9. References

[1] C. Cauzzi, J. Clinton, A high-and low-noise model for high-quality strong-motion accelerometer stations, Earthq. Spectra. 29 (2013) 85-102.

[2] J. Havskov, G. Alguacil, Instrumentation in earthquake seismology, in: Anonymous Springer, 2016, pp. 13-100.

[3] E. Wielandt, Seismic sensors and their calibration, in: M. Korn (Ed.), *Ten Years of German Regional Seismic Network (GRSN)*, Report 25 of the Senate Commission for Geosciences, , Wiley-VCH Verlag GmbH, Weinheim, Germany, 2002.

[4] J. Brownjohn, Structural health monitoring of civil infrastructure, Philos. Trans. A. Math. Phys. Eng. Sci. 365 (2007) 589-622.

[5] H. Lam, F. Zhang, Y. Ni, J. Hu, Operational modal identification of a boat-shaped building by a Bayesian approach, Eng. Struct. 138 (2017) 381-393.

[6] S. Au, F. Zhang, Ambient modal identification of a primary–secondary structure by Fast Bayesian FFT method, Mech. Syst. Signal Process. 28 (2012) 280-296.

[7] S. Kavitha, R.J. Daniel, K. Sumangala, High performance MEMS accelerometers for concrete SHM applications and comparison with COTS accelerometers, Mechanical Systems and Signal Processing. 66 (2016) 410-424.

[8] P.L. Reu, D.P. Rohe, L.D. Jacobs, Comparison of DIC and LDV for practical vibration and modal measurements, Mechanical Systems and Signal Processing. 86 (2017) 2-16.

[9] MG Beker, XH Campman, R. van Es, D. Chavan and A. Bertolini. Instrumental Noise Measurement of Seismic Sensors with a Sub-ng Vibration Isolation System. In: 77th EAGE Conference and Exhibition 2015. Madrid, Spain. 01-04 Jun, 2015.

[10] J. Brownjohn, T. Botfield, A folded pendulum isolator for evaluating accelerometer performance, Exp Tech. 33 (2009) 33-37.

[11] A. Barzilai, T. VanZandt, T. Kenny, Technique for measurement of the noise of a sensor in the presence of large background signals, Rev. Sci. Instrum. 69 (1998) 2767-2772.

[12] G.L. Pavlis, F.L. Vernon, Calibration of seismometers using ground noise, Bull. Seism. Soc. Am. 84 (1994) 1243-1255.

[13] J. Peterson, C.R. Hutt, L.G. Holcomb, Test and calibration of the seismic research observatory, US Geol. Surv. Open-File Rept. (1980) 80-187.

[14] L.G. Holcomb, A direct method for calculating instrument noise levels in side-by-side seismometer evaluations, U.S. Geol. Surv. Open-File Rept. (1989) 89-214.

[15] J.R. Evans, F. Followill, C.R. Hutt, R. Kromer, R. Nigbor, A. Ringler, J. Steim, E. Wielandt, Method for calculating self-noise spectra and operating ranges for seismographic inertial sensors and recorders, Seismol. Res. Lett. 81 (2010) 640-646.

[16] A. Ringler, R. Sleeman, C.R. Hutt, L.S. Gee, Seismometer self-noise and measuring methods, in: M. Beer, I. A. Kougioumtzoglou, E. Patelli, and S.-K. Au (Ed.), *Encyclopedia of Earth- Quake Engineering*, Springer, Berlin/Heidelberg, Germany, 2014, pp. 3220-3231.

[17] R. Sleeman, A. Van Wettum, J. Trampert, Three-channel correlation analysis: a new technique to measure instrumental noise of digitizers and seismic sensors, Bull. Seism. Soc. Am. 96 (2006) 258-271.

[18] C.R. Hutt, J.R. Evans, F. Followill, R.L. Nigbor, E. Wielandt, Guidelines for standardized testing of broadband seismometers and accelerometers, US Geol.Surv.Open-File Rept. 1295 (2009) 62.

[19] A. Ringler, J.R. Evans, C.R. Hutt, Self-noise models of five commercial strong-motion accelerometers, Seismol. Res. Lett. 86 (2015) 1143-1147.

[20] A. Ringler, C. Hutt, Self-noise models of seismic instruments, Seismol. Res. Lett. 81 (2010) 972-983.

[21] X. Li, D. Yang, J. Xie, J. Ma, S. Yuan, W. Xu, J. Zhao, D. Li, Applicability of the Welch method for examining self-noise level parameters for broadband seismometers, J. Geodes. Geodyn. 6 (2015) 233-239.

[22] J.M.W. Brownjohn, S. Au, Y. Zhu, Z. Sun, B. Li, J. Bassitt, E. Hudson, H. Sun, Bayesian operational modal analysis of Jiangyin Yangtze River Bridge, Mech. Syst. Signal Process. 110 (2018) 210-230.

[23] D. Hester, J. Brownjohn, M. Bocian, Y. Xu, A. Quattrone, Using inertial measurement units originally developed for biomechanics for modal testing of civil engineering structures, Mech. Syst. Signal Process. 104 (2018) 776-798.

[24] L.G. Holcomb, A numerical study of some potential sources of error in side-by-side seismometer evaluations, U.S. Geol. Surv. Open-File Rept. (1990) 90-406.

[25] A. Gerner, G. Bokelmann, Instrument self-noise and sensor misalignment, Adv Geosci. 36 (2013) 17-20.

[26] A. Ringler, C. Hutt, J. Evans, L. Sandoval, A comparison of seismic instrument noise coherence analysis techniques, Bull. Seism. Soc. Am. 101 (2011) 558-567.

[27] R. Sleeman, P. Melichar, A PDF representation of the STS-2 self-noise obtained from one year of data recorded in the Conrad Observatory, Austria, Bull. Seism. Soc. Am. 102 (2012) 587-597.

[28] Darren Hart, John Merchant and Eric P. Chael. Seismic and infrasound sensor testing using three-channel coherence analysis. In: 29th monitoring research review: ground-based nuclear explosion monitoring technologies. Denver, Colorado. 25-27 Sep, 2007.

[29] I. Tasič, F. Runovc, Seismometer self-noise estimation using a single reference instrument, J. Seismol. 16 (2012) 183-194.

[30] A. Gerner, R. Sleeman, W. Lenhardt, B. Grasemann, Improving Self-Noise Estimates of Broadband Seismometers by 3D Trace Rotation, Seismol. Res. Lett. 88 (2016) 96-103.

[31] P. Welch, The use of fast Fourier transform for the estimation of power spectra: a method based on time averaging over short, modified periodograms, IEEE Transactions on audio and electroacoustics. 15 (1967) 70-73.